

Carbon loss from aboveground woody debris generated through land conversion from a secondary peat swamp forest to an oil palm plantation

Takashi HIRANO^{a,†}, Guan Xhuan WONG^b, Joseph Wenceslaus WAILI^b, Kim San LO^b, Frankie KIEW^b, Edward Baran AERIES^b, Ryuichi HIRATA^c, Kiwamu ISHIKURA^{a,d}, Masato HAYASHI^e, Shoko MURATA^{a,f}, Tomohiro SHIRAIISHI^e, Masayuki ITOH^g and Lulie MELLING^b

^aResearch Faculty of Agriculture, Hokkaido University, Sapporo 060-8589, Japan

^bSarawak Tropical Peat Research Institute, Lot 6035, 94300 Kota Samarahan, Sarawak, Malaysia

^cCenter for Global Environmental Research, National Institute for Environmental Studies, Tsukuba 305-8506, Japan

^dTokachi Agricultural Experiment Station, Hokkaido Research Organization, Memuro 082-0081, Japan

^eEarth Observation Research Center, Japan Aerospace Exploration Agency, Tsukuba 305-8505, Japan

^fJapan Science and Technology Agency, Kawaguchi 332-0012, Japan

^gSchool of Human Science and Environment, University of Hyogo, Himeji 670-0092, Japan

Abstract

Palm oil accounts for about 40% of the global demand of vegetable oil. To meet the demand, oil palm plantations have expanded in the humid tropics at the expense of tropical forests. Land conversion begins with clear cutting and generates much woody debris, which was stacked in rows. Woody debris decomposes and emits carbon dioxide (CO₂), but the time course of the decomposition is not well understood, especially at the early stage. Thus, we measured carbon (C) stock in woody debris in a newly established plantation after clear cutting of a secondary peat swamp forest in Sarawak, Malaysia. A litter bag method was applied to examine the decomposition of woody debris scattered on the ground. Also, we periodically measured apparent cross-sectional area (ACSA) of a stacking row (about 5 m wide and 90 m long) assuming that the cross-sectional form was triangular. The C stock of the stacking row was estimated from ACSA and measured C fractions using a significant sigmoidal relationship. The decomposition rate constants (*k*) for C content were determined to be 0.231–0.313 yr⁻¹ for ground woody debris and 0.459 yr⁻¹ for stacked woody debris. In addition, the total decomposition of the aboveground woody debris proceeded according to another *k* of 0.440 yr⁻¹ during the experimental period of 740 days. The total C stock of aboveground woody debris was 48.4 Mg C ha⁻¹ at the beginning of the field experiment, about 16 months after clear cutting. The C stock accounted for 63% of the C of forest aboveground biomass. Despite the uncertainty in the spatial representativeness, we think that simply measurable ACSA is useful to quantify the C stock of stacked woody debris. The technique could be applicable to large-area estimation using drone technology.

Key words: Apparent cross-sectional area, Biomass, CO₂ emissions, Decomposition rate constant (*k*), Stacking row

1. Introduction

Palm oil accounts for about 40% of the current global demand of vegetable oil because oil palm can grow on various types of soils, have low maintenance costs, and have high yield (Dislich *et al.*, 2017; Meijaard *et al.*, 2020). Thus, oil palm plantations have expanded in the humid tropics that have the optimum climate for oil palm cultivation. In 2019, oil palm plantations covered at least 19.5 Mha globally, of which 90% was in Southeast Asia, especially Malaysia and Indonesia (Descals *et al.*, 2021). Much of plantation expansion has come at the expense of tropical forests, which are rich in biodiversity and carbon.

Land conversion of forests into plantations begins with clear cutting. Zero burning of residue is mandatory, but controlled burning can be still conducted to minimize the propagation of pests and diseases and the incidence of wildfires upon approval from the local authority (Harun *et al.*, 2011). Although some wood is sometimes extracted for local use, most woody matter, consisting of trunks, branches, twigs, stumps, and coarse roots, is usually left as woody debris and stacked in line along harvesting rows to improve work efficiency (Dolmat, 2005; Harun *et al.*, 2011). Because loss through burning and extracting is limited, the amount of woody debris left in plantations basically depends on forest biomass before clear cutting. In peatlands, drains are excavated for water management, and peat soil is mechanically compacted for increasing soil bulk density to minimize leaning and toppling of palm trees and increase soil moisture holding capacity. After such land preparation, saplings are planted.

Mass of woody debris decreases as decomposition proceeds. The decomposition losses arise from three processes: leaching, fragmentation, and chemical alteration (Chapin *et al.*, 2011). Leaching transfers soluble materials away from debris.

Received; February 2, 2022

Accepted; June 28, 2022

†Corresponding author: hirano@env.agr.hokudai.ac.jp

DOI: 10.2480/agrmet.D-22-00003



© Author (s) 2022.
This is an open access article
under the CC BY 4.0 license.

Fragmentation physically breaks large pieces into smaller ones. Chemical alteration of debris results primarily from microbial respiration (heterotrophic respiration), mineralizing organic matter into carbon dioxide (CO₂), which dominates the decomposition losses. For instance, respiratory CO₂ emissions accounted for 76% of total carbon (C) loss through coarse woody debris (CWD) decomposition in Central Amazon forests (Chambers *et al.*, 2001). Woody debris decomposes complexly, depending on substrate size, vertical position (downed vs. standing), chemical quality, temperature, moisture, and microbial species (Harmon *et al.*, 2011); decomposition proceeds faster in downed debris than standing one because downed debris has higher accessibility of decomposers and higher moisture. Heterotrophic respiration showed a positive correlation with moisture (Chambers *et al.*, 2001) but would be suppressed by oxygen scarcity in moisture saturation (Song *et al.*, 2017). Also, burning affects decomposition. Because charred woody material due to burning is low in decomposition (DeLuca and Aplet, 2008), it is important to count charred CWD for assessing the carbon balance of postfire ecosystems (Donato *et al.*, 2009).

The time course of woody debris decomposition is not well understood (Harmon *et al.*, 2020), especially for tropical forests (Giardina, 2019). Thus, to elucidate dynamic variation in the CO₂ balance of young plantations converted from forest, it is essential to quantify the time course of CO₂ emissions from a large amount of stacked woody debris (McCalmont *et al.*, 2021). Some field studies reported the *k* of woody debris from field experiments in tropical or subtropical mature forests (Chambers *et al.*, 2001; Yang *et al.*, 2010; Song *et al.*, 2017), but these *k* values would be inapplicable to young plantations, mainly because environmental conditions of woody debris are basically different. In young plantations, stacked woody debris would

have less contact with the ground and be directly exposed to solar radiation, probably resulting in higher temperature and lower moisture (Forrester *et al.*, 2015).

In this study, we periodically measured the amount of mass and C of stacked woody debris for about two years in a young oil palm plantation established after clear cutting to assess the time course of woody debris decomposition. The objectives of this study are 1) to determine the *k* value of whole woody debris left in the plantation, 2) to quantify the time course of woody debris C stock, 3) to quantify C loss and CO₂ emissions through the decomposition of woody debris, and 4) to discuss the applicability of the approach we applied.

2. Material and Methods

2.1. Study site

The study site was a young oil palm plantation (1°23'59"N, 111°24'7"E, 17 m above sea level) in Sarawak, Malaysia, converted from a secondary peat swamp forest (Fig. 1a) with the canopy height of 25 m (Kiew *et al.*, 2018). The forest had been selectively logged until the 1980s and regenerated as a secondary forest. Originally, the forest was dominated by *Shorea albida*, but *Lithocarpus bancanus* and *Litsea crassifolia* became dominant through succession.

Trees were clear-cut and left on the ground as well as drain construction in June–August 2017 (Fig. 1b) and had been dried by the sun, and then partially burned in February 2018 (Fig. 1c). The remaining woody debris after burning was stacked in a row (stacking row) in the middle of each plot, and the ground was mechanically compacted, according to the guideline of Malaysian Palm Oil Board (Harun *et al.*, 2011). In May 2018, oil palm seedlings were planted in a triangular pattern with 8.5 m spacing (Fig. 1d). The peat depth was 5.4–7.2 m in 2018 after

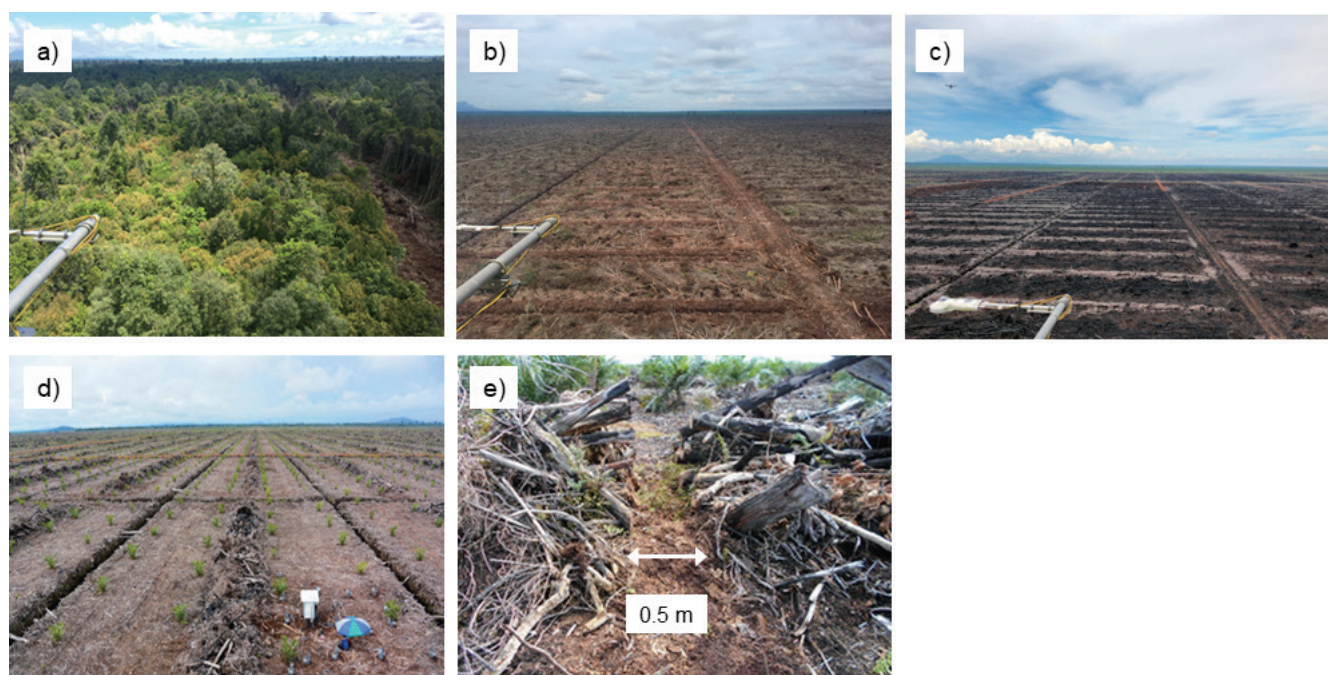


Fig. 1. Time-series photos of the study site: a) May 2017 (a construction road is seen at the right end), b) October 2017, c) March 2018, d) June 2018, and e) November 2018.

plantation establishment. Mean annual precipitation and air temperature were 2665 ± 305 mm yr⁻¹ and 26.5 ± 0.2 °C (mean \pm standard deviation (SD)) from 2011 through 2020 at the flux tower in the site (Kiew *et al.*, 2018). In the study period, annual precipitation was 2381, 2756, and 2564 mm yr⁻¹, respectively, in 2018, 2019, and 2020, which were within the range of mean \pm 1 SD of the decadal records. Generally, precipitation is lower in July–August and higher in December–January in this region with relatively unclear seasonal variation (Wong *et al.*, 2018).

2.2. Forest carbon stock

A field survey was conducted in July 2017 (just before clear cutting) in four plots of 30 m \times 40 m around the flux tower (Kiew *et al.*, 2018) to assess the initial C stock before land conversion. For every tree with diameter at breast height (DBH) > 5 cm, the scientific name was recorded, and DBH and tree height were measured, respectively, using a measuring tape and ultrasonic range finder (Vertex IV, Haglöf Sweden AB, Långsele, Sweden). Trees were classified into 28 species in total. Aboveground biomass (AGB) and belowground biomass (BGB) were calculated from DBH, tree height, and wood density using allometric equations (Table 5 in Monda *et al.*, 2015); Model 2 for AGB and Model 6 for BGB. The allometric equations had been determined from field data in a peat swamp forest near our study site, considering stem hollows, which are common in peat swamp trees in Sarawak (Monda *et al.*, 2018). Wood density information of each species was collected from literatures (Brown, 1997; Monda *et al.*, 2015) and a dataset (Zanne *et al.*, 2009). Biomass was converted into C using a factor of 0.464 (Murdiyarso *et al.*, 2009).

All dead wood > 5 cm in diameter was collected in the forest and grouped into five decomposition classes (Law *et al.*, 2008), but classes 1 and 2 were combined (1–2) because of their small sample sizes. Length and diameter of each sample were measured, and the volume was estimated as a cylinder. From each class, four or five sub-samples were collected and dried at 80°C until reaching constant weight to measure dry matter, and then wood density was calculated. In addition, C and nitrogen (N) fractions were determined with a CN analyzer (TruMac CN,

Leco, St. Joseph, MI, USA). Bark was not separated from wood in the analysis. The C content was calculated from the volume, wood density, and C fraction (Table 1).

2.3. Carbon stock in ground woody debris

Most woody debris was stacked (stacked woody debris), though some smaller ones were scattered on the ground (ground woody debris). No leaf litter was visually found. On November 29, 2018, ground woody debris was collected from five quadrats of 1 m \times 1 m and weighed and classified into three groups: large (L) > 8 cm, medium (M) > 3 cm, and small (S) > 1 cm in diameter. The classes of L and M plus S correspond to CWD and fine woody debris (FWD), respectively (Law *et al.*, 2008). Most ground woody debris had no burn mark. Six sub-samples were collected from each size and dried at 80°C to measure dry matter and water fraction. Also, C and N fractions were determined with a CN analyzer (TruMac CN, Leco). Using the mean water and C fractions for each size, mass and C content of each sample were calculated from its fresh weight, and then they were summed up.

Decomposition was examined using litter bags. Woody samples were collected randomly regardless of tree species and classified into the three size-categories. Cylindrical pieces of about 150 g of total fresh weight were put into a 2-mm meshed plastic bag (24 cm \times 40 cm). We prepared 30 bags for each size. The bags were divided into five groups, and each group from the three sizes was installed all together on the sunny ground in the plantation on November 29, 2018. Thus, the bags were exposed to solar radiation, which potentially heated and desiccated woody debris in the bags during the daytime. One bag was sampled from each group for each size, meaning 18 bags were sampled in total on each date in March, July, November 2019, May, and July 2020. Samples were weighed before and after oven-drying to determine dry weight and water fraction. In addition, C and N fractions of every sample were analyzed by the same method described above. The decomposition rate constant k (d⁻¹) was determined by fitting the following equation to the data.

$$Y/Y_0 = \exp(-k \cdot t) \quad (1)$$

Table 1. Density, carbon (C) fraction, and nitrogen (N) fraction of woody debris in four decomposition classes in a secondary peat swamp forest in July 2017 just before clear cutting (mean \pm SD, $n = 4-5$).

Class	Wood density	C fraction	N fraction	Remarks
	Mg m ⁻³	g C g DM ⁻¹	mg N g DM ⁻¹	
1	0.511 \pm 0.039	48.0 \pm 0.37	0.0978 \pm 0.0222	The wood is solid and there has been very little decay.
2				Logs that have lost almost all of the fine branches.
3	0.480 \pm 0.169	47.7 \pm 0.93	0.118 \pm 0.081	Usually losing the bark and beginning to loose portions of sapwood.
4	0.289 \pm 0.105	49.6 \pm 0.96	0.102 \pm 0.056	Logs have lost the ability to support themselves but still have a round to elliptical shape rising above the general forest floor.
5	0.418 \pm 0.076	51.2 \pm 0.97	0.310 \pm 0.138	Form the ill-defined hummocks that appear to be part of the forest floor.

* Classes 1 and 2 were combined because of the small sample size.

where Y is the weight of dry matter or C remaining in bags (g bag^{-1}) at elapsed time t (days) and Y_0 the initial dry weight of samples (g bag^{-1}), which was 90.5, 80.8, and 70.8 g bag^{-1} , respectively, for L, M, and S sizes.

2.4. Carbon stock in stacked woody debris

One stacking row was formed in every plot of about 100 m \times 30 m (three plots per hectare) (Fig. 1d). Stacking rows had rectangular plane shapes of about 90 m \times 5 m. To estimate the dry matter and C stock, we measured cross-sectional dimensions and analyzed C fraction of a stacking row near the flux tower.

Although the cross-sectional shape was irregular, it was assumed to be triangular (Fig. 2), because the cross section looks like a triangle rather than a quadrangle and an arc. In addition, the triangle is simple and practical, because it is determined only by width and height (Fig. 2). We set 22 points at intervals of 4 m along the long side, excluding 1 m from each end. At every point, width and height of the cross section were measured with a measuring tape and range finder (Vertex IV, Haglöf Sweden AB), respectively, in November 2018, May, November 2019, May, and December 2020. Apparent cross-sectional area (ACSA) was calculated from the width and height, and then the apparent volume of the row was calculated by multiplying mean ACSA by a fixed length of 90 m. Also, at other randomly selected five points, all woody debris were sampled in 0.5 m thickness using a chain saw (Fig. 1e) as well as measuring ACSA in November 2018, May, November 2019, and May 2020. All samples were classified into six groups (three sizes \times two burning conditions (burned and unburned)) and weighed in the field, though burned samples of S size were hardly found. Most of burned samples were only charred on the outside. On each date, six sub-samples

were collected randomly regardless of tree species from each group, and their water, C, and N fractions were analyzed by the same method described above. For burned samples, charred outside was included in the analysis. In each group, the dry matter of all samples was calculated from fresh weight measured in the field and the water fraction of sub-samples measured in the laboratory. In addition, C content of all samples was estimated in each group from the dry matter and C fraction of sub-samples, and then the C content was summed over the groups in each of five 0.5-m-thick bands.

2.5. Statistical analysis

We applied one-way and two-way repeated measures ANOVA to test the effects of debris size and burning conditions on C and N fractions. The significance of linear and curve fitting was tested using F -test, respectively. All the statistical analyses were conducted using a software package (OriginPro 2021b; Origin Lab Corporation, Northampton, MA, USA).

3. Results

3.1. Biomass and woody debris before clear cutting

Biomass and woody debris before clear cutting were 198 and 43.0 Mg ha^{-1} , respectively; AGB accounted for 83% of total biomass (Table 2). We expected the biomass and woody debris were left as plant debris, including leaves, just after clear cutting. The C stocks of biomass and woody debris were 91.9 and 21.8 Mg C ha^{-1} , respectively. Top seven species accounted for 83% of total AGB and 84% of total tree numbers (Table 3). Woody debris grouped into classes 1–2, 3, 4, and 5 (Table 1) accounted for 3, 5, 15, and 77% of the total woody debris C, respectively. As a result, the total plant C of 114 Mg C ha^{-1}

Table 2. Carbon (C) contents of biomass and woody debris in a secondary peat swamp forest in July 2017 just before clear cutting.

Plot	Tree density trees ha^{-1}	AGB Mg ha^{-1}	BGB Mg ha^{-1}	Total biomass Mg ha^{-1}	AGB C ¹⁾ Mg C ha^{-1}	BGB C ²⁾ Mg C ha^{-1}	Total biomass C Mg C ha^{-1}	Woody debris Mg ha^{-1}	Woody debris C Mg C ha^{-1}	Total C Mg C ha^{-2}
1	2258	114	23.0	137	53.0	10.7	63.7	10.3	5.2	68.9
2	1842	180	33.7	213	83.3	15.6	98.9	38.2	19.4	118.4
3	2458	148	27.4	176	68.9	12.7	81.6	66.6	33.8	115.4
4	2067	216	50.4	266	100.0	23.4	123.4	56.9	28.7	152.1
Mean \pm SD	2156 \pm 228	164 \pm 37.4	33.6 \pm 10.4	198 \pm 47.5	76.3 \pm 17.4	15.6 \pm 4.8	91.9 \pm 22.0	43.0 \pm 21.5	21.8 \pm 10.9	114 \pm 29.6

¹⁾ Calculated from AGB using a factor of 0.464 (Murdiyarto *et al.*, 2009).

²⁾ Calculated from BGB using a factor of 0.464 (Murdiyarto *et al.*, 2009).

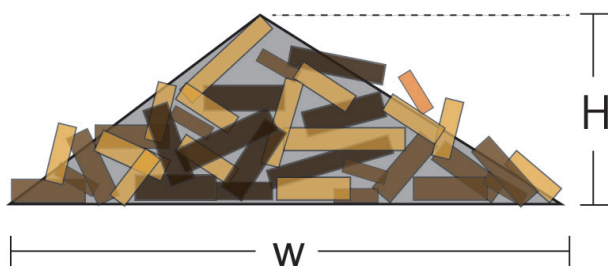


Fig. 2. Schematic diagram of a cross-sectional shape approximated by a triangle (W: width, H: height).

Table 3. Shares (%) of top seven tree species in aboveground biomass (AGB) and tree number.

Species	AGB	Number
<i>Lithocarpus bancanus</i> Rehder	33.4	27.3
<i>Litsea crassifolia</i> (Blume) Boerl.	11.5	13.2
<i>Combretocarpus rotundatus</i> Danser	10.0	7.8
<i>Syzygium</i> spp.	8.8	14.9
<i>Dactylocladus stenostachys</i> Oliver	7.6	6.9
<i>Aglaiia leptantha</i> Miq.	5.9	11.6
<i>Shorea albida</i> Sym.	5.7	2.0

existed in the site (Table 2).

The dominant tree species changed to *Lithocarpus bancanus* (Table 3) from original *Shorea albidia*, which usually dominates intact peat swamp forests in this area (Monda *et al.*, 2015). Because the conversion of intact forests is strictly inhibited, woody debris originating from disturbed forests like this secondary forest with a different tree composition from the original would be typically left in newly developed plantations.

3.2. Carbon stock in ground woody debris

Total dry mass of 9.28 ± 4.54 Mg ha⁻¹ (mean \pm SD) was left on the ground on November 29, 2018. The corresponding C stock was 4.24 ± 2.13 Mg C ha⁻¹; L, M, and S size classes accounted for 41, 38, and 21%, respectively.

The Eq. 1 was significantly fitted to each size for both dry mass and C content ($p < 0.001$, Fig. 3). The annual k values were 0.252 ± 0.067 (L), 0.405 ± 0.061 (M), and 0.319 ± 0.054 (S) yr⁻¹ (mean \pm standard error (SE)) for dry mass and 0.231 ± 0.069 (L), 0.313 ± 0.058 (M), and 0.260 ± 0.052 (S) yr⁻¹ for C content. Both C and N fractions significantly increased during the experiment (Fig. 4). No significant difference was found among sizes in both C and N fractions ($p > 0.05$). The C/N ratio showed a linear trend only in S size ($p < 0.001$), which decreased from 309 ± 36 to 99 ± 33 (mean \pm SD) in 606 days. Water fractions were 0.400 ± 0.060 (L), 0.480 ± 0.101 (M), and 0.483 ± 0.121 (S) g g⁻¹ with no significant trend for all sizes.

3.3. Carbon stock in stacked woody debris

In 740 days, the width and height of the stacking row significantly decreased ($p < 0.001$) from 5.6 to 5.0 m (Fig. 5a) and 1.76 to 1.00 m (Fig. 5b), respectively. As a result, ACSA linearly decreased ($p < 0.001$) from 4.75 ± 0.26 to 2.54 ± 0.19 m² by 47% in 740 days (Fig. 5c).

The C fraction significantly increased in all sizes for unburned (U) samples ($p < 0.001$), but not for burned (B) ones (Fig. 6a).

Variation in C fraction among sub-samples was small on each sampling date; coefficients of variance (CV) ranged between 1.6% (unburned small: US) and 4.2% (burned medium: BM) on average. In contrast, N fraction significantly increased for B samples ($p < 0.01$), but not for U samples (Fig. 6b). As a result, US, BM, and burned large (BL) samples showed linear increases in C/N ratio ($p < 0.01$). Water fractions showed no significant trend in all sizes with means between 0.416 (BL) and 0.541 g g⁻¹ (BM). Two-way repeated measures ANOVA showed significant differences between burning conditions in both C and N fractions, but no difference among sizes; C and N fractions were greater in B ($p < 0.001$ for C and $p = 0.013$ for N). There were no significant differences in C/N ratio and water fraction.

The C contents of woody debris (per ground area of 1 m²) sampled from 0.5-m-thick bands were 34.8 ± 10.9 (November 2018), 20.0 ± 5.4 (May 2019), 34.7 ± 7.9 (November 2019), and 9.9 ± 3.8 (May 2020) kg C m⁻² (mean \pm SD, $n = 5$). Corresponding dry matter was 67.9 ± 20.7 , 39.4 ± 11.2 , 63.0 ± 14.1 , and 18.2 ± 7.0 kg m⁻², respectively. The relationships of C content (Y_c , kg C m⁻²) and dry matter (Y_d , kg m⁻²) with ACSA (X_A , m²) were significantly fitted by the following sigmoidal equations ($p < 0.001$, $r^2 = 0.694$ for C and $p < 0.001$, $r^2 = 0.741$ for dry matter) (Fig. 7).

$$Y_c = \frac{55.2}{1 + 19.6 \cdot e^{-0.682 \cdot X_A}} \quad (2)$$

$$Y_d = \frac{103}{1 + 22.9 \cdot e^{-0.728 \cdot X_A}} \quad (3)$$

The Y_c on each measurement date was calculated from mean ACSA (Fig. 5c) using Eq. 2, and then the total C stock (Mg C ha⁻¹) of stacked woody debris was calculated as the product of mean Y_c , mean width, the fixed stacking row length (90 m), and the density of stacking rows (3 rows ha⁻¹) (Fig. 8). In 740 days, C stock decreased by 60% from 45.4 to 18.3 Mg C ha⁻¹. Daily C loss rates decreased by 70% from 55.3 kg C ha⁻¹ d⁻¹

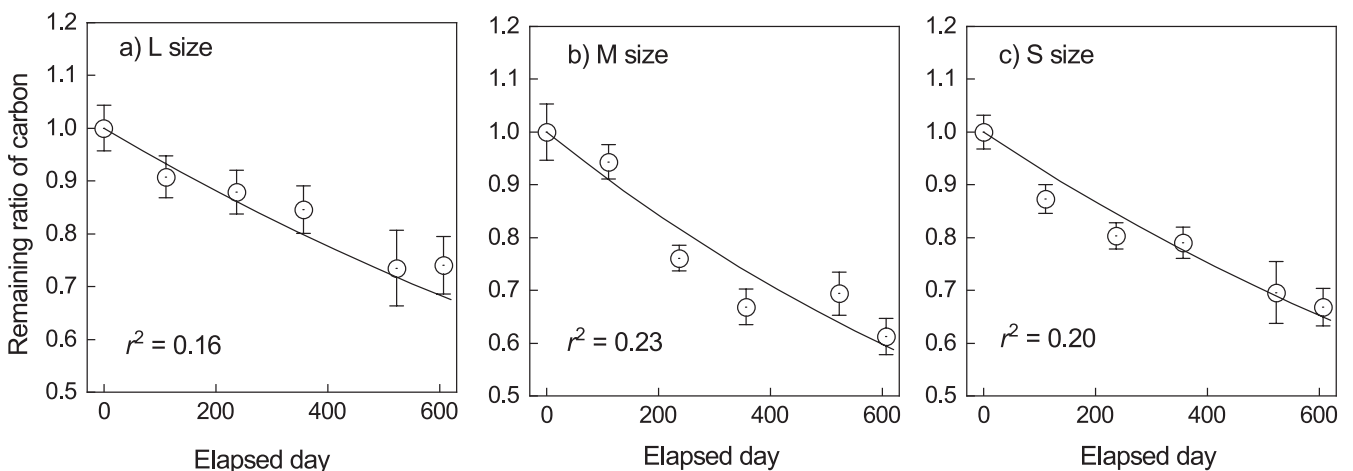


Fig. 3. Temporal changes in the remaining ratio of carbon content of woody debris in litter bags from November 2018, in L (a), M (b), and S (c) size classes. Mean \pm standard error (SE) is shown ($n = 6$). A negative exponential equation (Eq. 1) is significantly ($p < 0.001$) fitted for each size of woody debris, respectively.

in the first period between November 2018 and May 2019 to 16.7 kg C ha⁻¹ d⁻¹ in the last period between May 2020 and December 2020. The relationship of C stock (*y*) with elapsed days (*x*) was significantly approximated by Eq. 1 ($p < 0.001$, Fig. 8): $y = 44.2 \times \exp(-0.00126 \times x)$ ($r^2 = 0.988$); the annual *k* was determined to be 0.459 yr⁻¹ from this equation and indicates that stacked woody C decreased to 10% in five years.

3.4. Change in aboveground wood debris C stock

Daily C stocks in ground and stacked woody debris were simulated (Fig. 9) using the *k* values during the experiment (0.231–0.313 yr⁻¹ for ground debris (Fig. 3) and 0.459 yr⁻¹

for stacked debris (Fig. 8)). Daily aboveground total C stock was calculated as the sum of estimated ground and stacked C stocks, and its time course was approximated using Eq. 1. As a result, the *k* of 0.440 yr⁻¹ was determined for aboveground total C stock of woody debris. During the period of 740 days, total C stock decreased by 59% from 48.4 Mg C ha⁻¹ in November 2018 to 19.9 Mg C ha⁻¹ in December 2020 at an average rate of 38.5 kg C ha⁻¹ d⁻¹.

4. Discussion

A secondary peat swamp forest with total C of 115 Mg C ha⁻¹ (Table 1) was converted into an oil palm plantation. The forest

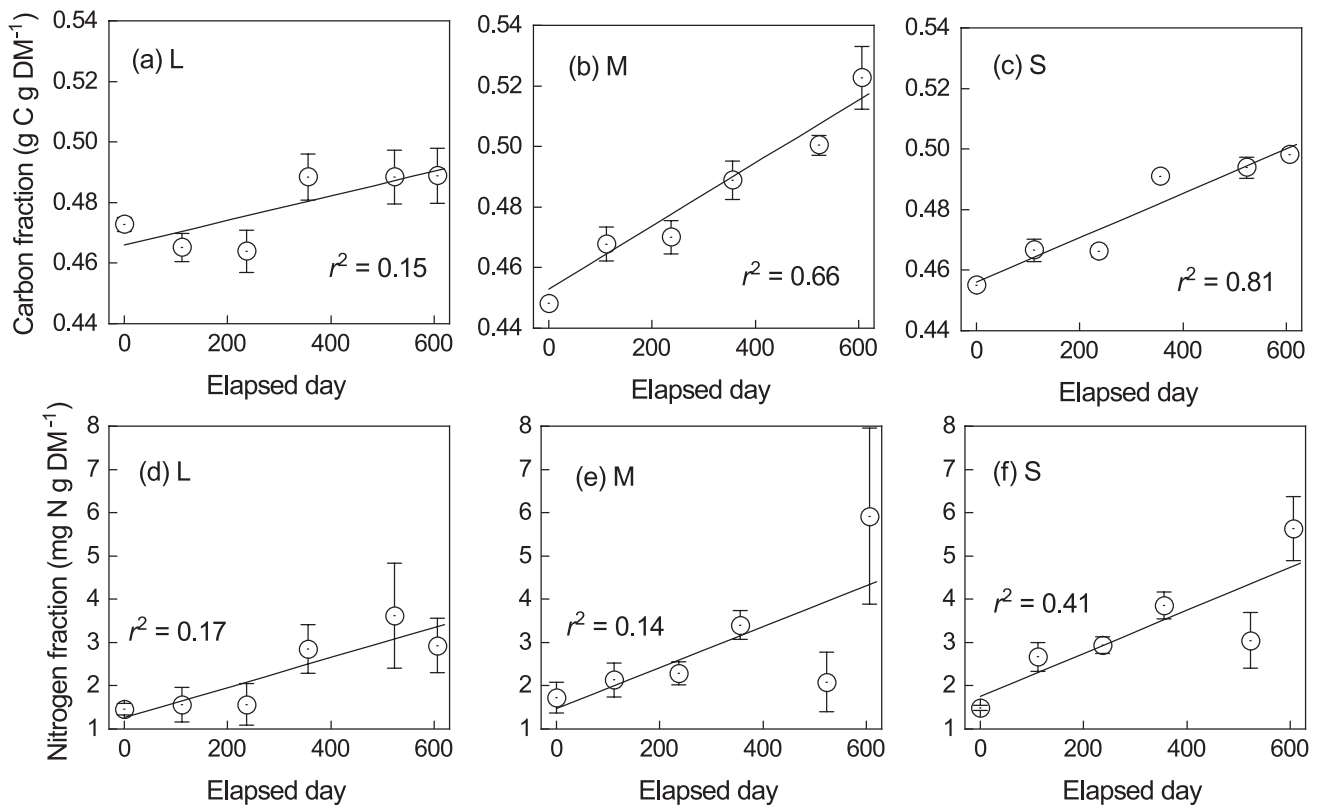


Fig. 4. Temporal changes in carbon fraction (a–c) and nitrogen fraction (d–f) of woody debris in litter bags from November 2018, in L, M, and S sizes. Mean \pm standard error (SE) is shown ($n = 6$). Significant positive correlation was found in all panels ($p < 0.05$).

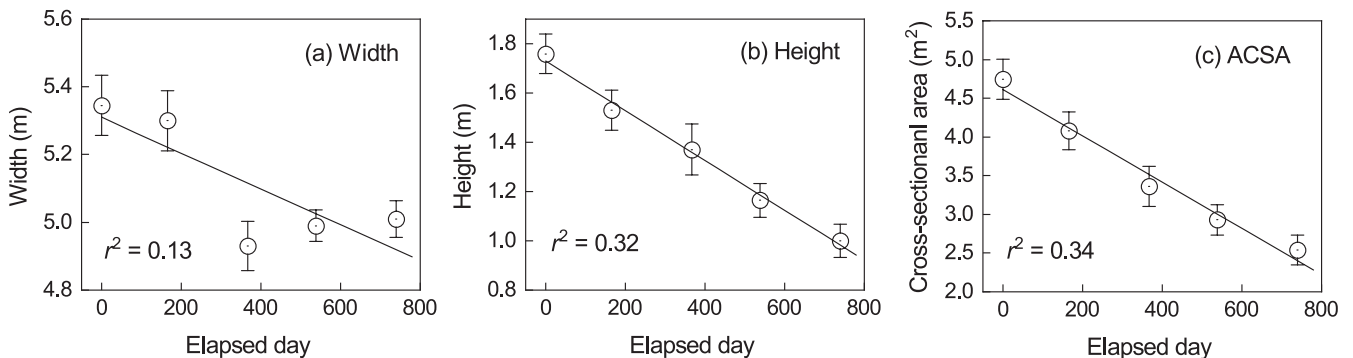


Fig. 5. Temporal changes in width (a), height (b), and apparent cross-sectional area (ACSA) (c) of a stacking row from November 2018. Mean \pm standard error (SE) is shown ($n = 22$). Significant negative correlation was found in all panels ($p < 0.001$).

C stock was 47% of that of relatively undisturbed peat swamp forests in Southeast Asia (Verwer and van der Meer, 2010), and the forest AGB was 86% of the average over Borneo (Hayashi *et al.*, 2015).

Woody debris was scattered on the ground and stacked through plantation establishment, and decreased exponentially according to the rate constant k . The k values tended to be higher for FWD than for CWD (Berg and McClaugherty, 2014). Meanwhile, it was reported that woody debris with smaller diameter has lower k in dry conditions, such as in open space (Harmon *et al.*, 2011), but such water limitation was unlikely

to happen in this study even on the ground, because low water fractions were not measured probably owing to relatively humid climate conditions. There are a few studies on CWD decomposition in tropical and subtropical forests; reported k values for dry mass were 0.015–0.67 yr⁻¹ in mature forests in Central Amazon (Chambers *et al.*, 2000) and Southern China (Yang *et al.*, 2010; Song *et al.*, 2017). Our k value for CWD dry matter (0.252 yr⁻¹ for L size) was compatible with the reported values, though they varied widely.

During the experiment, C and N fractions increased on the ground (Fig. 3). Such a C increase was explained by temporal

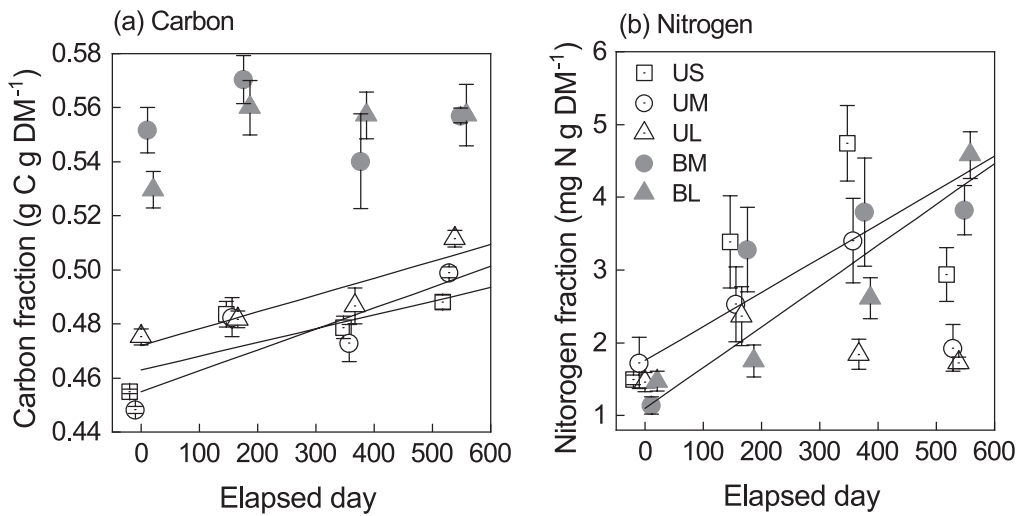


Fig. 6. Temporal changes in carbon fraction (a) and nitrogen fraction (b) of woody debris in a stacking row from November 2018. Mean \pm standard error (SE) is shown ($n=6$). Significant positive correlation was found for unburned samples (U) in carbon fraction (a) and burned samples (B) in nitrogen fraction (b) ($p < 0.01$), respectively.

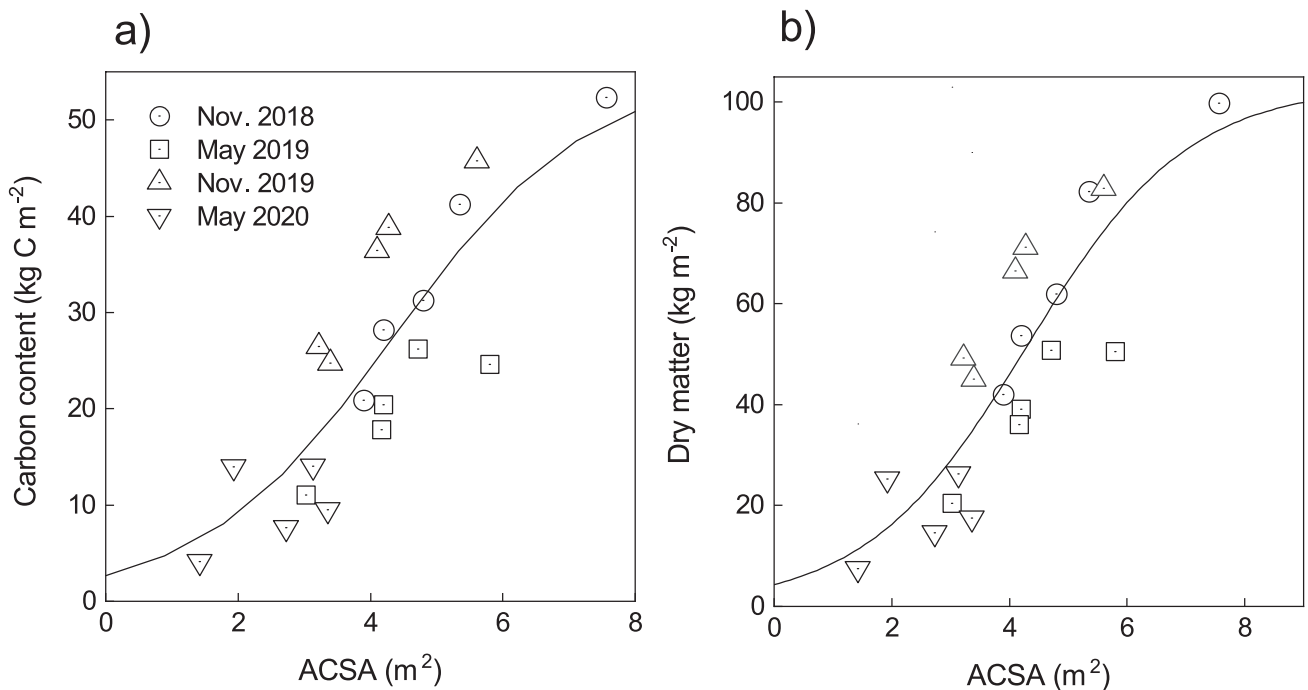


Fig. 7. Relationships of carbon content (a) or dry matter (b) of collected woody debris and apparent cross-sectional area (ACSA). Sigmoidal equations (Eqs. 2 and 3) were significantly fitted, respectively ($p < 0.001$).

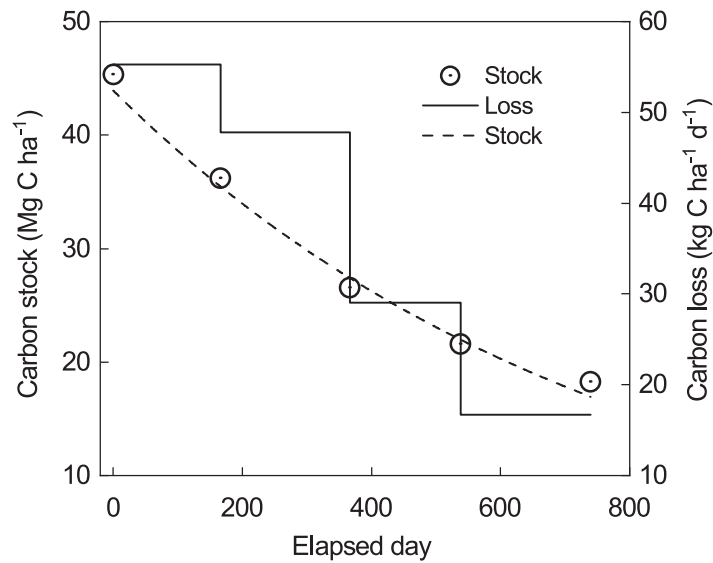


Fig. 8. Temporal change in carbon stock in the whole stacking row from November 2018. Carbon stock was estimated from mean ACSA using Eq. 2. Daily carbon loss was also calculated from the stock change. A negative exponential equation (Eq. 1) was significantly fitted ($p < 0.001$).

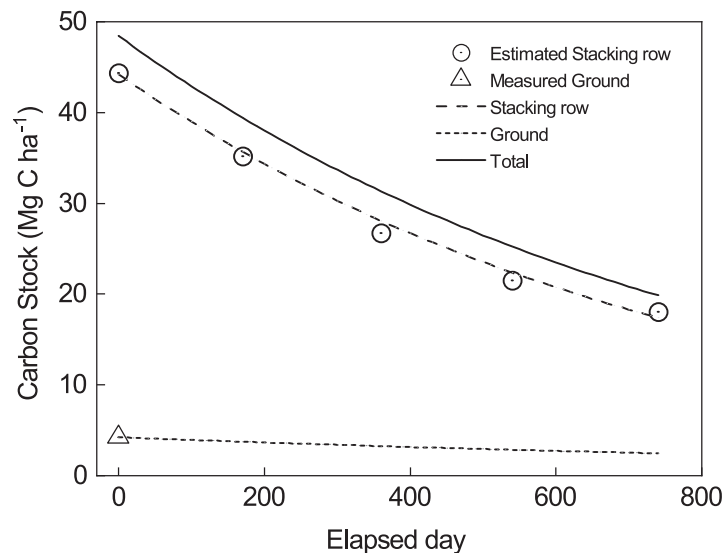


Fig. 9. Temporal change in the carbon stock of aboveground woody debris during the experimental period from November 2018 to December 2020. Daily carbon stock on the ground and in a stacking row were simulated using k values (Figs. 3 and 8), respectively, and their sum is also shown as Total. Measured carbon stock on the ground was shown as an open triangle. Carbon stocks in a stacking row estimated from mean ACSA using Eq. 2 were shown as open circles.

change in woody debris composition, resulting from different decomposition rates of cellulose/hemicellulose with a lower C fraction and lignin with a higher C fraction (Martin *et al.*, 2021; Romashkin *et al.*, 2021). Because cellulose/hemicellulose decomposes faster than lignin, C fraction can increase with time. The N increase was common and would be due to the growth of microbial biomass, N_2 fixation and atmospheric deposition (Cornwell *et al.*, 2009; Romashkin *et al.*, 2021). In the stacking row, C fraction increased only in unburned samples (Fig. 6). Burned samples were analyzed together with charred parts.

Because char has a higher C fraction than unburned materials and is recalcitrant (DeLuca and Aplet, 2008), the C fraction of burned samples was higher and almost stable.

Since logs were irregularly stacked, there was much interspace initially. We expected that the interspace was easily crushed in the early stages, causing a rapid decrease in ACSA for small decomposition. Thus, we applied a sigmoidal function to model the relationships of cross-sectional C content and dry matter with ACSA (Fig. 7). From mean ACSA, we estimated the C stock of the whole stacking row using Eq. 2, which

explained the spatiotemporal variation of C content by 69% ($r^2 = 0.694$). As a result, the C stock exponentially decreased according to a k of 0.459 yr^{-1} (Fig. 8). The k value of stacked woody debris was higher than that of ground woody debris, probably because of termites. Termites have a significant impact on wood decomposition, especially in the tropics (Cornwell *et al.*, 2009). Woody debris was burned only on the outside. Thus, wood-feeding termites should have survived the fire. We found traces of termites only in the stacking row. In Sumatra, Indonesia, termites were also found in burned trees (Neoh *et al.*, 2016).

The aboveground total C stock of woody debris was estimated to be $48.4 \text{ Mg C ha}^{-1}$ at the beginning of the field experiment (Fig. 9), about 16 months after clear cutting. Although the C stock resulted from a single site of 0.3 ha with no replication, the C stock accounted for 63% and 49%, respectively, of AGB ($76.3 \text{ Mg C ha}^{-1}$) and AGB plus woody debris ($98.1 \text{ Mg C ha}^{-1}$) before clear cutting (Table 2). In Sarawak, annual ecosystem respiration of an oil palm plantation converted from a peat swamp forest was $35.2 \text{ Mg C ha}^{-1} \text{ yr}^{-1}$ in the 7–10th years after establishment (Kiew *et al.*, 2020). From the k value of 0.440 yr^{-1} for aboveground total C stock (Fig. 9) and a conversion factor (0.76) of CO_2 emission (respiration) from C loss (decomposition) (Chambers *et al.*, 2001), annual CO_2 emissions from the aboveground woody debris ($98.1 \text{ Mg C ha}^{-1}$) in the seventh and tenth years were calculated to be 1.89 and $0.51 \text{ Mg C ha}^{-1} \text{ yr}^{-1}$ in our site, respectively, which accounts for 5.4% and 1.4% of the ecosystem respiration ($35.2 \text{ Mg C ha}^{-1} \text{ yr}^{-1}$). In the same plantation as in Kiew *et al.* (2020), annual CO_2 emission through peat decomposition was measured to be $6.9 \text{ Mg C ha}^{-1} \text{ yr}^{-1}$ in the 11–12th years (Ishikura *et al.*, 2018). The CO_2 emissions through aboveground woody debris decomposition in our site in the same years account for 3–5% of the peat decomposition. The comparisons indicate that the contribution of aboveground woody debris decomposition would become minor in ecosystem CO_2 emissions in a decade or so.

The significant sigmoidal equation (Eq. 2) with higher r^2 indicates triangular apparent cross-sectional area (ACSA) would be an effective proxy for stacked woody C stock (Fig. 7a). Small variation in the C fraction of sub-samples on each sampling date (Fig. 6a) suggests that the sub-sampling ensured the representativeness within a stacking row and supports the utility of ACSA. Using Eq. 2, we quantified C stock and C loss (Fig. 8) and determined the inclusive k of 0.440 yr^{-1} for aboveground total woody debris (Fig. 9). Meanwhile, since the results came from a single stacking row, there was uncertainty in the spatial representativeness. However, the relationship between C content and ACSA (Fig. 7a) would be robust, because samples were extracted from variously sized cross sections even on the same sampling date. The variances in cross-sectional dimensions of within a row and among rows were possibly at the same level. In addition, CO_2 emissions calculated from C loss would have another uncertainty. Although all C loss is assumed to be simultaneously emitted to the atmosphere as CO_2 in many studies (e.g., Eggeston *et al.*, 2006; McCalmont *et al.*, 2021), part of the C moves into the soil and water as organic compounds. Most of the organic compounds should be eventually mineralized into CO_2 , but it was much later and in different places (Regnier *et al.*, 2013; Wit *et al.*, 2015). Thus, CO_2 emissions are potentially overestimated under the assumption. To avoid it, we applied a conversion factor of 0.76 (Chambers *et al.*, 2001). However, uncertainty remains in the factor because it depends on the decomposing stage, decomposers' species, and substrate size (Chambers *et al.*, 2001). Despite the uncertainty in the spatial representativeness and conversion factor, we believe that simply measurable ACSA is useful to quantify the C stock of stacked woody debris. The technique could be applicable to large-area estimation using aerial approaches, such as drone technology.

Acknowledgements

This study was supported by JSPS Bilateral Open Partnership Joint Research Projects, JSPS KAKENHI Grant Number JP19H05666, Research Institute for Humanity and Nature (RIHN, Project No. 14200117) and Sarawak State Government. We thank the Sarawak Tropical Peat Research Institute for the valuable advice and assistance in this study. We also thank the supporting staff (Kevin Dinggun Kanang, Felix Axel Seli, Gan Haip and Evefilanwell Frederick) and Chemistry Division of Sarawak Tropical Peat Research Institute for their assistance in the field work and samples analysis.

References

- Berg B, McClaugherty C, 2014: *Plant Litter: Decomposition, Humus Formation, Carbon Sequestration* (Third Edition), Springer-Verlag, Berlin, pp. 322.
- Brown S, 1997: Estimating Biomass and Biomass Change of Tropical Forests: a Primer. *FAO Forestry Paper*, <https://www.fao.org/3/w4095e/w4095e00.htm>.
- Chambers JQ, Higuchi N, Schimel JP *et al.*, 2000: Decomposition and carbon cycling of dead trees in tropical forests of the central Amazon. *Oecologia* **122**, 380–388.
- Chambers JQ, Schimel JP, Nobre AD, 2001: Respiration from coarse wood litter in central Amazon forests. *Biogeochemistry* **52**, 115–131.
- Chapin FS III, Matson PA, Vitousek PM, 2011: Decomposition and Ecosystem Carbon Budgets. In *Principle of terrestrial ecosystem ecology, Second Edition*, Springer, New York, pp. 183–228.
- Cornwell WK, Cornelissen JHC, Allison SD *et al.*, 2009: Plant traits and wood fates across the globe: rotted, burned, or consumed? *Global Change Biology* **15**, 2431–2449.
- DeLuca TH, Aplet GH, 2008: Charcoal and carbon storage in forest soils of the Rocky Mountain West. *Frontiers in Ecology and the Environment* **6**, 18–24.
- Descals A, Wich S, Meijaard E *et al.*, 2021: High-resolution global map of smallholder and industrial closed-canopy oil palm plantations. *Earth System Science Data* **13**, 1211–1231.
- Dislich C, Keyel AC, Salecker J *et al.*, 2017: A review of the ecosystem functions in oil palm plantations, using forests as a reference system. *Biological Reviews* **92**, 1539–1569.
- Dolmat MT, 2005: Technologies for Planting Oil Palm on Peat. Malaysian Palm Oil Board, pp. 84.
- Donato DC, Campbell JL, Fontaine JB *et al.*, 2009: Quantifying char in postfire woody detritus inventories. *Fire Ecology* **5**, 104–115.
- Eggeston S, Buendia L, Miwa K *et al.*, 2006: 2006 IPCC Guidelines for National Greenhouse Gas Inventories,

- <https://www.ipcc-nggip.iges.or.jp/public/2006gl/>.
- Forrester JA, Mladenoff DJ, D'amato AW *et al.*, 2015: Temporal trends and sources of variation in carbon flux from coarse woody debris in experimental forest canopy openings. *Oecologia* **179**, 889–900.
- Giardina CP, 2019: Advancing Our Understanding of Woody Debris in Tropical Forests. *Ecosystems* **22**, 1173–1175.
- Harmon ME, Bond-Lamberty B, Tang J *et al.*, 2011: Heterotrophic respiration in disturbed forests: A review with examples from North America. *Journal of Geophysical Research* **116**, G00K04, doi:10.1029/2010JG001495.
- Harmon ME, Fash BG, Yatskov M *et al.*, 2020: Release of coarse woody detritus-related carbon: a synthesis across forest biomes. *Carbon Balance Management* **15**, 1–21.
- Harun MH, Kushairi A, Mohammed AT *et al.*, 2011: Guidelines for the Development of a Standard Operating Procedure for Oil Palm Cultivation on Peat. Malaysian Palm Oil Board, pp. 9.
- Hayashi M, Saigusa N, Yamagata Y *et al.*, 2015: Regional forest biomass estimation using ICESat/GLAS spaceborne LiDAR over Borneo. *Carbon Management* **6**, 19–33.
- Ishikura K, Hirano T, Okimoto Y *et al.*, 2018: Soil carbon dioxide emissions due to oxidative peat decomposition in an oil palm plantation on tropical peat. *Agriculture Ecosystems & Environment* **254**, 202–212.
- Kiew F, Hirata R, Hirano T *et al.*, 2018: CO₂ balance of a secondary tropical peat swamp forest in Sarawak, Malaysia. *Agricultural and Forest Meteorology* **248**, 494–501.
- Kiew F, Hirata R, Hirano T *et al.*, 2020: Carbon dioxide balance of an oil palm plantation established on tropical peat. *Agricultural and Forest Meteorology* **295**, 108189.
- Law BE, Arkebauer T, Campbell JL *et al.*, 2008: Terrestrial Carbon Observations: Protocols for Vegetation Sampling and Data Submission. Global Terrestrial Observing system, Rome, pp. 87.
- Martin AR, Domke GM, Doraisami M *et al.*, 2021: Carbon fractions in the world's dead wood. *Nature Communication* **12**, 889, <https://doi.org/10.1038/s41467-021-21149-9>.
- McCalmont J, Kho LK, Teh YA *et al.*, 2021: Short- and long-term carbon emissions from oil palm plantations converted from logged tropical peat swamp forest. *Global Change Biology* **27**, 2361–2376.
- Meijaard E, Brooks TM, Carlson KM *et al.*, 2020: The environmental impacts of palm oil in context. *Nature Plants* **6**, 1418–1426.
- Monda Y, Kiyono Y, Chaddy A *et al.*, 2018: Association of growth and hollow stem development in *Shorea albida* trees in a tropical peat swamp forest in Sarawak, Malaysia. *Trees* **32**, 1357–1364.
- Monda Y, Kiyono Y, Melling L *et al.*, 2015: Allometric equations considering the influence of hollow trees: A case study for tropical peat swamp forest in Sarawak. *Tropics* **24**, 11–22.
- Murdiyarso D, Donato D, Kauffman JB *et al.*, 2009: Carbon storage in mangrove and peatland ecosystems: A preliminary account from plots in Indonesia. CIFOR, Bogor, pp. 35.
- Neoh KB, Bong LJ, Muhammad A *et al.*, 2016: The impact of tropical peat fire on termite assemblage in Sumatra, Indonesia: Reduced complexity of community structure and survival strategies. *Environmental Entomology* **45**, 1170–1177.
- Regnier P, Friedlingstein P, Ciais P *et al.*, 2013: Anthropogenic perturbation of the carbon fluxes from land to ocean. *Nature Geoscience* **6**, 597–607.
- Romashkin I, Shorohova E, Kapitsa E *et al.*, 2021: Substrate quality regulates density loss, cellulose degradation and nitrogen dynamics in downed woody debris in a boreal forest. *Forest Ecology and Management* **491**, 119143.
- Song Z, Dunn CL, Lü XT *et al.*, 2017: Coarse woody decay rates vary by physical position in tropical seasonal rainforests of SW China. *Forest Ecology and Management* **385**, 206–213.
- Verwer C, van der Meer P, 2010: Carbon pools in tropical peat forest – Towards a reference value for forest biomass carbon in relatively undisturbed peat swamp forest in Southeast Asia. *Alterra-report 2108*, Wageningen, pp. 64.
- Wit F, Muller D, Baum A *et al.*, 2015: The impact of disturbed peatlands on river outgassing in Southeast Asia. *Nature Communions* **6**, 10155, DOI: 10.1038/ncomms10155.
- Wong GC, Hirata R, Hirano T *et al.*, 2018: Micrometeorological measurement of methane flux above a tropical peat swamp forest. *Agricultural and Forest Meteorology* **256-257**, 353–361.
- Yang FF, Li YL, Zhou GY *et al.*, 2010: Dynamics of coarse woody debris and decomposition rates in an old-growth forest in lower tropical China. *Forest Ecology and Management* **259**, 1666–1672.
- Zanne AE, Lopez-Gonzalez G, Coomes DA *et al.*, 2009: Data from: Towards a worldwide wood economics spectrum, Dryad, Dataset, <https://doi.org/10.5061/dryad.234>.